

Rapid characterization of emulsions by pulsed field gradient nuclear magnetic resonance

*Geir Humborstad Sørland¹, Serkan Keleşoğlu², Sébastien Simon²
and Johan Sjöblom²*

¹Anvendt Teknologi AS, Trondheim Norway (www.antek.no)

²Ugelstad Laboratory, Department of Chemical Engineering, the Norwegian University of Science and Technology, Trondheim Norway

(received 01 February 2013, received in revised form 18 February 2013,
available online 20 February 2013)

Abstract

A method for rapid characterization of emulsions is presented. From the proposed set-up we are able to measure the droplet size distribution of brine or water droplets confined by an oil phase, even though there is complete overlap in relaxation times and/or molecular mobility between the water and the oil phases. A PFG-NMR sequence is presented that applies the spoiler recovery method for significant reduction in acquisition time, and the method is used for rapid characterization of emulsions.

Keywords: Pulsed field gradient, emulsions, NMR, diffusion, relaxation, acquisition time, recycle delay

1. Introduction

The use of PFG-NMR for the characterization of emulsions was introduced by Stejskal and Tanner back in [1-2]. Since this initial work on restricted diffusion, the method has been further developed into a broad range of applications to characterize various food emulsions [3-6] and crude oil emulsion [7]. However, most of the methods have been based on the work by Packer and Rees [8] with the basic assumption that the shape of the distribution follows a log-normal distribution [3, 6, 9-12]. Such an assumption certainly puts an important restriction on the method, as for example bimodal emulsion systems will not fit into this category of distributions. This also goes for the assumption of a mono exponential decay with respect to the longitudinal relaxation time for the oil phase. The latter prevents us from applying this method for emulsions based on crude oils where the relaxation components may vary several orders of magnitude. Peña and Hirasaki [13] included a CPMG sequence to avoid the a priori assumption of a defined shape of the distribution. But they still applied the same diffusion model as used by Packer and Rees to find the droplet sizes, thus not being particularly applicable to crude oil emulsion systems. Aichele et al [7] presented a technique using PFG-NMR with diffusion editing (DE) to quantify brine/crude oil emulsions. This technique made no assumptions on the distribution shape. However, each measurement was relatively long, 5-7 hours, and proved sensitive to coalescence. Recently Bernewitz et.al provided a thorough survey on methods for measuring droplet sizes by NMR [14].

Opedal et.al [15] presented recently a method for the characterization of the emulsions that does not contain the restrictions as mentioned above. It is just as sensitive to a log-normal distribution as to a bimodal droplet size distribution, it does not assume a mono exponential longitudinal relaxation decay of the oil phase, and it is quite rapid as it takes approximately 5 minutes to conduct the experiment. Their methods are based on the possibility of suppressing the crude oil signal due to a significant difference in longitudinal relaxation time. Sørland et.al [16] introduced the spoiler recovery method, which further reduced the acquisition time, disregarding the need for a waiting time of 5 times T_1 between each scan. This method initially spoils the magnetization to have zero net magnetization in any direction, and it has shown to apply for magnetic field strength from 0.5 to 11.6 Tesla [17-18]. Currently the state of the art is to measure droplet size distributions of brine in oil system within a minute, without any a priori expectation of the shape of the distribution.

In the following we will deduce how we transfer a T_2 to a droplet size distribution (DSD), provide the combined spoiler recovery pulsed field gradient sequences used for extracting the DSD , and verify the NMR results against microscopy.

2. Theory

2.1 Extracting droplet size distribution from water in oil emulsions

As shown by Packer et.al [14], there is a situation where the surface relaxation term is absent in the solution of the diffusion propagator [19], i.e. for diffusion within closed cavities and when the diffusing molecules have covered mean free path lengths \gg cavity dimension $[(6 D_0 t)^{1/2} \gg R_{cavity}]$. In such a situation the attenuation of the NMR signal from diffusion within the closed droplet can be simplified to [14] [20]

$$\frac{I}{I_0} \approx \exp \left[-\frac{\gamma^2 \delta^2 g^2 R^2}{5} \right] \quad (2.1)$$

where δ is the gradient pulse length, g is the applied gradient strength and R is the droplet radius. In a heterogeneous system a distribution in droplet sizes must be assumed. As long as $[(6 D_0 t)^{1/2} \gg R_{cavity}]$ holds for all sizes eq. (2.1) is valid also for a heterogeneous system. If ξ_i is the volume fraction of the droplets with surface to volume ratio $(S/V)_i$, eq. (2.1) can be expressed as

$$\frac{I}{I_0} \approx \sum_i \xi_i \exp \left[-\frac{\gamma^2 \delta^2 g^2 R_i^2}{5} \right] \quad (2.2)$$

When the exponent in Equation 2.2 is small for all i , we may expand the exponential functions using its two first terms:

$$\frac{I}{I_0} \approx \left(\sum_i \xi_i - \sum_i \xi_i \frac{\gamma^2 \delta^2 g^2 R_i^2}{5} \right) = 1 - \frac{\gamma^2 \delta^2 g^2 \overline{R^2}}{5} \quad (2.3)$$

Where $\overline{R^2}$ yields the average value of the square of the droplet radius. Measurements of the early departure from I_0 as a function of applied gradient strength may then result in a value for the average surface to volume ratio. This can be used in combination with a T_2 distribution to result in a droplet size distribution as shown in the following.

Assuming that the water molecules are probing the droplets within the sample, there is a simple relation [21] between T_2 values and the droplet sizes

$$T_2 \approx \frac{V}{S\rho} \quad (2.4)$$

This couples the surface to volume ratio to the surface relaxivity, ρ , and makes it difficult to assign the T_2 distribution directly to a (V/S) distribution. However, if we make the assumption that eq. (2.4) holds for any droplet size, with ξ_i being the volume fraction of pores with surface to volume ratio $(S/V)_i$ and corresponding relaxation time T_{2i} , we may follow Uh and Watson [22] and write

$$\sum_i \xi_i \frac{1}{T_{2i}^2} = \sum_i \xi_i \rho_i^2 \left(\frac{S}{V} \right)_i^2 = 9 \sum_i \xi_i \rho_i^2 \left(\frac{1}{R_i^2} \right) \approx 9 \rho^2 \left(\overline{\frac{1}{R^2}} \right) \quad (2.5)$$

Here we have made the assumption that the surface relaxivity ρ is independent of droplet size. The left hand side of eq. (2.5) is the harmonic mean $\overline{1/T_2}$ of the T_2 -distribution weighted by the fraction ξ_i of nuclei with relaxation time T_{2i} and n is the number of subdivisions of droplet sizes. This average can be calculated from the T_2 -distribution obtained in a CPMG measurement where the magnetization attenuation $M^{obs}(t)$ is converted to a T_2 distribution by solving an inverse problem using e.g. an Inverse Laplace Transform (ILT) routine [23]. Then the surface relaxivity ρ can be calculated from eq. (2.5)

$$\rho = \frac{1}{3} \sqrt{\left(\overline{\frac{1}{T_2^2}} \right) \times \left(\overline{\frac{1}{R^2}} \right)^{-1}} \quad (2.6)$$

$\left(\overline{R^2} \right)$ is the quantity that we are able to measure according to equation 2.3. $\left(\overline{\frac{1}{R^2}} \right)^{-1}$ is a parameter that we have to find an expression for based on measurable quantities in order to find a value for the surface relaxivity. Again denoting (S/V) as $(3/R)$, as for spherical droplets and

assuming the surface relaxivity to be independent of droplet size we have the following relations

$$\left(\overline{\frac{1}{T_2}}\right) = 9\rho^2 \left(\overline{\frac{1}{R^2}}\right), \quad \overline{T_2^2} = \frac{\overline{R^2}}{9\rho^2}, \quad \text{and} \quad \left(\overline{\frac{1}{T_2}}\right) = 3\rho \left(\overline{\frac{1}{R}}\right) \quad (2.7)$$

From these expressions it's straight forward to deduce the following expression:

$$\left(\overline{\frac{1}{R^2}}\right) = \left(\overline{\frac{1}{T_2^2}}\right) \left(\overline{\frac{T_2^2}{R^2}}\right) \quad (2.8)$$

Substituting this in the equation for ρ we finally get

$$\rho = \frac{1}{3} \sqrt{\left(\overline{\frac{1}{T_2}}\right)^2 \left(\overline{\frac{T_2^2}{R^2}}\right)} \quad (2.9)$$

Finally, the measured T_2 -distribution can be transformed into an absolute droplet size distribution (I/S) by means of the relationship inherent in eq. (2.4). To sum up, the procedure for deriving absolute droplet size distributions is as follows:

- 1) The square of the average droplet radius is found from fitting eq. (2.1) to a diffusion measurement at long observation times.
- 2) The square of the average droplet radius can be correlated to the average (I/T_2) found from a CPMG experiment. From eq. (2.7) eq. (2.6) can then be written as

$$\left(\overline{\frac{1}{T_2}}\right) \approx 9\rho^2 \left(\overline{\frac{1}{R^2}}\right) \Rightarrow \rho = \frac{1}{3} \sqrt{\left(\overline{\frac{1}{T_2}}\right)^2 \left(\overline{\frac{T_2^2}{R^2}}\right)} \quad (2.10)$$

hence we find the relaxivity, ρ , which then is assumed to be droplet size independent.

- 3) Under the assumption of droplet size independency of the relaxivity the value of ρ can then be used in eq (2.6) thus resulting in a linear relation between T_2 and the volume to surface ratio which is a measure of the droplet size. By multiplying the T_2 distribution by the calculated surface relaxivity the distribution is normalized to a droplet size distribution in absolute length units

2.2 Separation of high viscosity crude oil and brine signal

There are several ways to separate the NMR contribution of the crude oil and brine components. The most straightforward way is when the viscosity of the crude oil is much higher than that of the brine phase. Then the longitudinal and/or the transverse relaxation times will be significant different, and one may store the NMR signal for full recovery of the crude oil signal back to thermal equilibrium while the brine signal still can be measured on. In figure 2.1 we have displayed the T_2 distributions of brine in crude oil emulsion system for short and long z-storage (Δ) intervals. By increasing the duration of the z-storage one can thus omit the oil signal. The two peaks at short Δ correspond to the oil signal (left peak) and water signal (right peak), which is the strategy used by Opedal et.al [15].

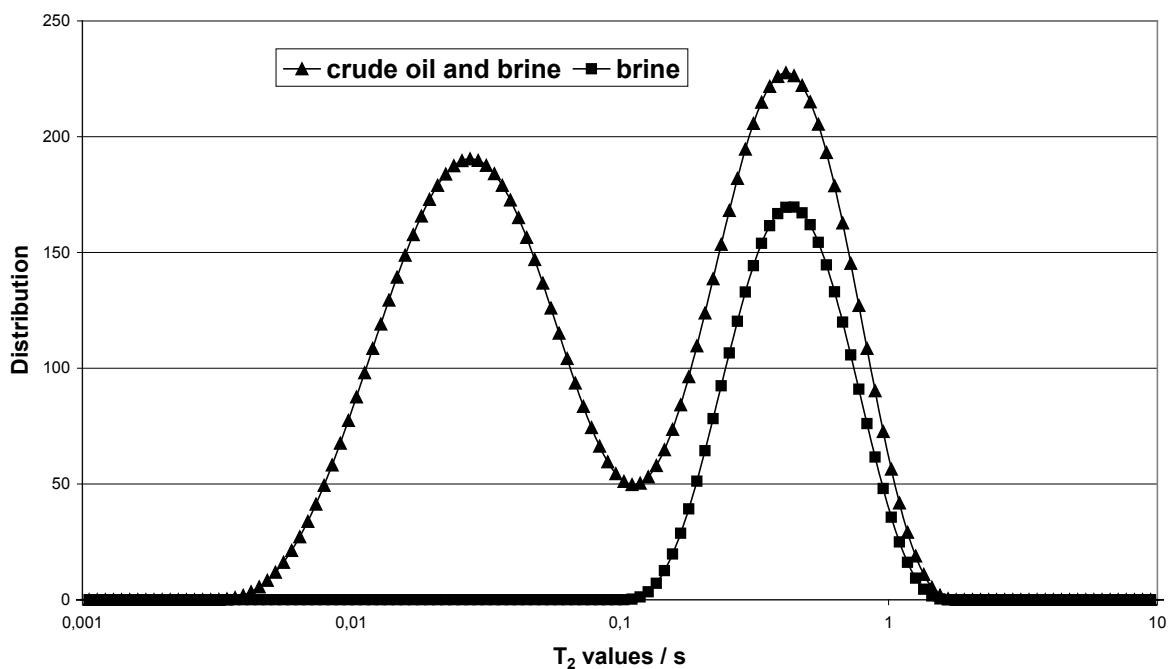


Figure 2.1: The effect of using z-storage delay Δ to obtain the T_2 distribution of brine alone.

2.3 Separation of low viscosity crude oil and brine signal

In systems where bulk brine is present, as in double emulsion; water droplets confined in oil droplets confined in a bulk water phase, or low viscosity oils where T_2 overlap with the T_2 's of the brine due to comparable viscosity, we have designed the following approach for measuring the DSD : As the root of the mean squared displacement (X) of the water confined in droplets is limited by the droplet size ($X_{DSD} \leq \text{droplet radius}$), the observation time in the convection compensated sequence in figure 3.1 is made so long that $X_{DSD} \ll X_{bulk}$, $X_{low\ viscosity\ oil}$. For example with Δ of 1 second the X of water at 25°C would be $\sim 100\mu\text{m}$. This will be much larger than the typical droplet diameter we report to be measured here, $\sim (1-20)\mu\text{m}$. In figure 2.2 it is shown how one may resolve the signal from the water inside the droplets from the water and/or low viscosity oil that move more freely. When the observation time is made so short that X_{bulk} , $X_{low\ viscosity\ oil} \approx X_{DSD}$, we will have a situation where we are not able to resolve the water confined in droplets from the bulk water or the low viscosity oil ('•' in figure 2.2), but as we increase the observation time we eventually arrive at the situation where $X_{DSD} \ll X_{bulk}$, $X_{low\ viscosity\ oil}$ ('+' in figure 2.2). Then we may easily resolve the water confined in droplets and measure the average squared droplet radius according to equation 2.3.

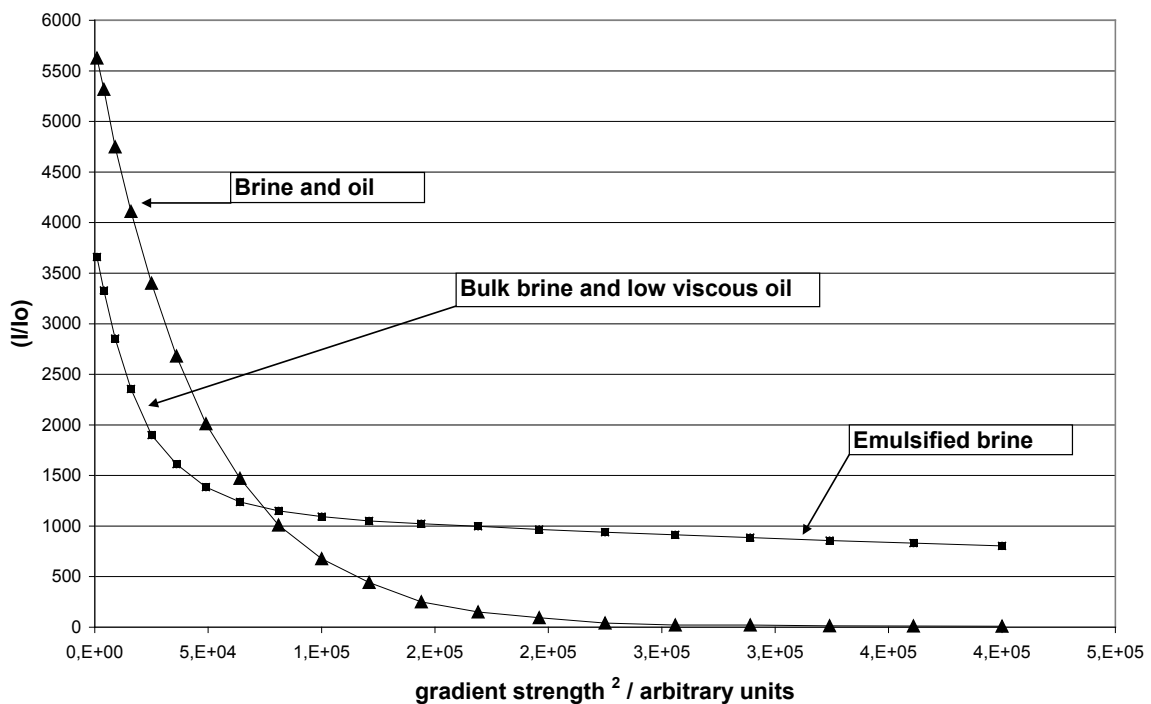


Figure 2.2: Resolving emulsified brine by increasing the observation time from short (▲) to long (■).

3. Experimental

3.1 The NMR experiments

The NMR experiments were performed on a 21 MHz benchtop NMR system supplied by Anvendt Teknologi AS and Advanced Magnetic Resonance. The gradient system has the ability of delivering approximately 400 G/cm at full power.

In figures 3.1-3.2 we have shown the sequences for suppressing bulk water and or the oil (regardless of viscosity), measuring the average squared droplet radius and the T_2 attenuation of the water confined in the droplets of the emulsion. The applied gradient pulse length used was 800 μ s and the τ -value in the 13-interval sequence was 1.5 ms.

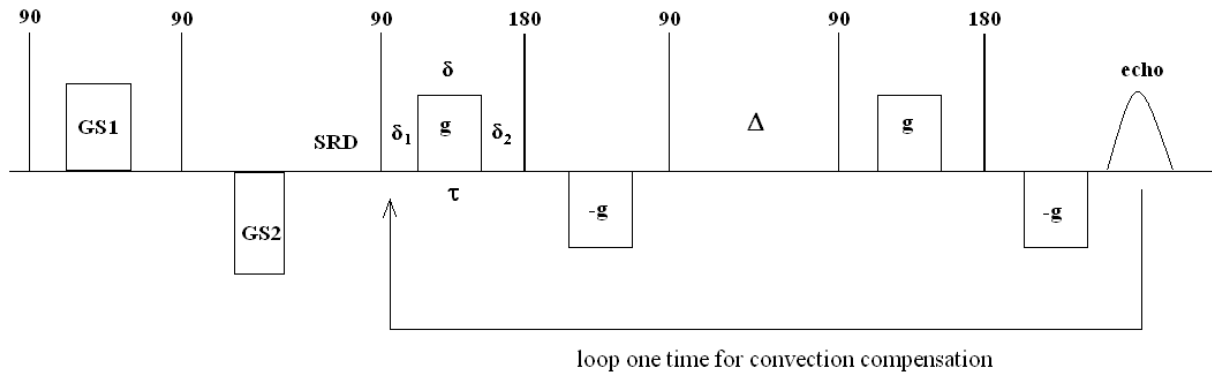


Figure 3.1. The combined spoiler recovery - 13 interval PFGSTE sequence with convection compensation

The corresponding attenuations for the sequence in figure 3.1 is written

$$I = I_0 e^{-2(\gamma^2 \delta^2 g^2 D_{(\Delta)} (\Delta + \frac{3\tau}{2} - \frac{\delta}{6}))} e^{-2(\frac{\Delta}{T_1} + \frac{4\tau}{T_2})} \quad (3.1)$$

where I_0 is the initial NMR signal intensity, γ is the gyromagnetic ratio, δ is the gradient pulse length, g is the strength of the gradient of the applied pulsed magnetic field, $D(\Delta)$ is the molecular diffusion coefficient, Δ is the z-storage delay, T_1 is the longitudinal relaxation time, T_2 is the transverse relaxation time and 2τ is the inter echo spacing.

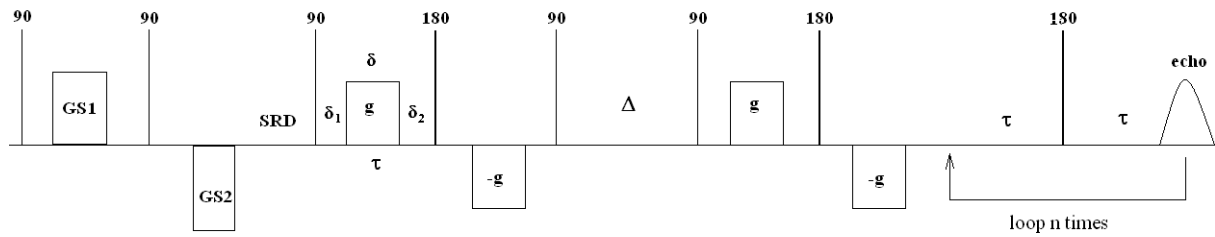


Figure 3.2. The combined spoiler recovery - 13 interval PFGSTE - CPMG sequence

The corresponding attenuations for the sequence in figure 3.1 is written

$$I = I_0 e^{-(\gamma^2 \delta^2 g^2 D_{(\Delta)} (\Delta + \frac{3\tau}{2} - \frac{\delta}{6}))} e^{-(\frac{\Delta}{T_1} + \frac{2n\tau}{T_2})} \quad (3.2)$$

where n is the echo number. The tool for performing a one dimensional inverse Laplace transform on the CPMG data was supplied by Anvendt Teknologi AS.

3.2 Preparation of Emulsions

The emulsions containing high viscosity oil were prepared by mixing the crude oils with water at room temperature (22°C), the total sample volume being 20 ml. As a mixer we applied an Ultra Turrax (Ika[®]-Werke Co., Germany) homogenizer (18 mm head) with a stirring speed of 20 000 rpm for 2 minutes. The emulsions with water cut of 30% were analyzed immediately after mixing.

The emulsion containing low viscosity oil was prepared by mixing the oil and water phases at the ambient temperature (22°C ± 1°C). The total volume of the emulsion was 10 ml and aqueous phase volume fraction of the emulsion was 0.30. 3 ml of Milli-Q water containing 3.5% NaCl and 7 mL of decane containing 2% (w/v) sorbiton sesquioleate (SPAN 83) were put into 25 ml glass tube and then mixed with Ultra Turrax (Ika[®]-Werke Co., Germany) using T25 with a 10 mm head at 24 000 rpm for 3 minutes. After the emulsification, the emulsions were correspondingly analyzed both with NMR and microscope.

3.3 Droplet Size Distribution Measured by Microscope

A Nikon Eclipse ME 600 digital video microscope with Image Pro Plus 5.0 software from Media Cybernetics and a CoolSNAP-Pro cfw 4 megapixel cooled CCD camera was used to determine droplet size distribution of the emulsion. The microscope contains the lens with the CFI LU Plan Epi 10 X with an numerical aperture of 0.30 and is capable of measuring the droplet size down to about 1 μm . Droplet size distribution of the emulsion was determined applying the following procedure: first the emulsion was diluted in the oil (1/20 (v/v)), because the original emulsion was too concentrated to separate and distinguish the droplets using the microscope, and 1–2 drop of the diluted emulsion placed on a glass slide. Afterward, the diluted emulsion was placed under the microscope and then several pictures were optimized and captured. The clusters and non-droplets were removed from the captured pictures and then the droplets were counted and the diameters were calculated using the Image Pro Plus 5.10 software. To obtain the distribution population of the droplets in the emulsion more than 300 droplets were chosen from the captured pictures and then analyzed.

4. Results and discussion

4.1 Droplet size distribution from a system containing high viscosity oil

One of the important features of the proposed method is that we are able to suppress the oil signal in two different ways, either by using a long observation time Δ , which is applicable for high viscosity oil samples and/or by applying strong enough magnetic pulsed field gradients in the 13 interval PFGSTE sequence, which is applicable for low viscosity oils. For oils with intermediate viscosity both effects will contribute to resolve the signal from water confined in the droplets from the oil signal.

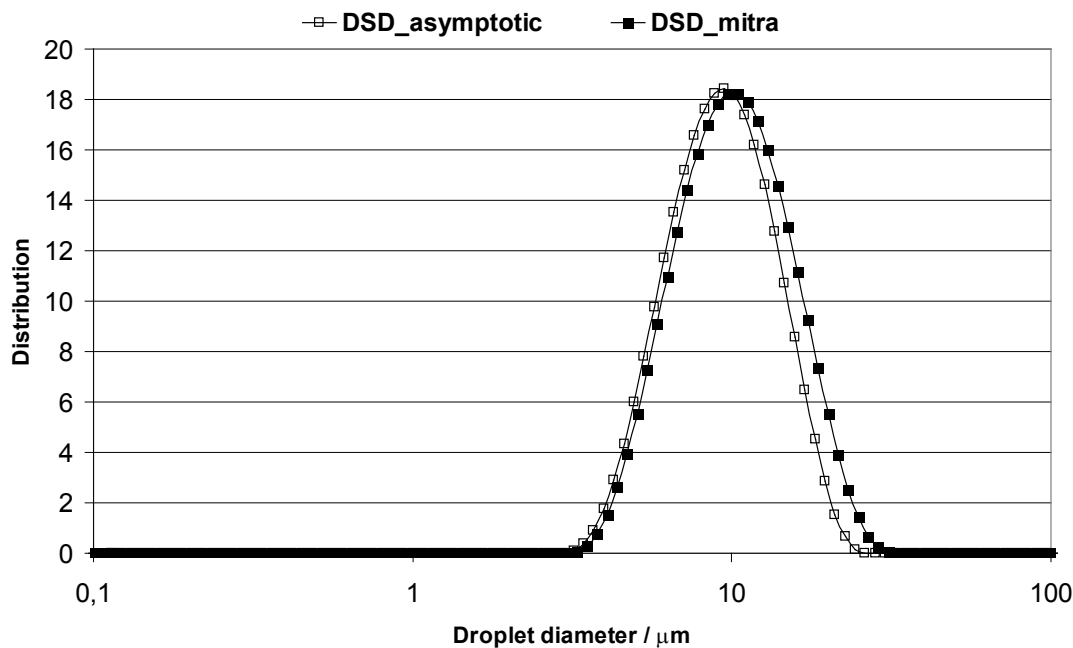


Figure 4.1: Comparison of the proposed method (*DSD_asymptotic*) against the method developed by Opedal et.al (*DSD_mitra*)

In figure 4.1 we have compared the method proposed here (*DSD_asymptotic*) against the method developed by Opedal et.al [15]. The system investigated was brine in crude oil emulsion with 30 % brine content/water cut, the very same as measured on by Opedal et.al [15]. The T_1 's of the crude oil were situated around 200 ms, so we could easily suppress the oil signal by using a Δ of 500 ms (i.e. $2\Delta=1$ second). The two droplet size distributions (*DSD*) are almost identical, and it confirms that both methods do measure the DSD quite accurately (*DSD_mitra* has already been validated against microscopy [15]).

4.2 Droplet size distribution from a system containing high viscosity oil

In figure 4.2 we show the results from an emulsion containing decane as the oil phase. In the bulk phase the decane is of practically the same viscosity as the bulk phase of the brine. Thus T_1 and T_2 's are overlapping, and we must combine relatively long Δ with magnetic field gradients to resolve the signal of the brine confined in the droplets ('■' in figure 2.2). The Δ used was 35 ms, but as the droplets were quite small, this observation time was sufficient to reach the asymptotic limit as given by Packer et.al (equation 2.1). When comparing with

microscopy we do find a reasonable agreement between the two methods. The *DSD* from the NMR method seems to be more broadened, but to get a sharper distribution from NMR it is just a matter of choosing the smoothing parameter in the inverse Laplace routine differently. However, as the microscopy arises from the counting of 306 droplets only and considering the fact that the droplet diameters are close to the resolution limit of the microscope, it is likely that the true *DSD* is broadened as shown by the NMR result. Most important is that the average droplet diameter from the two number based distributions are found to be quite similar, 1.5 μm from microscopy versus 1.8 μm from NMR.

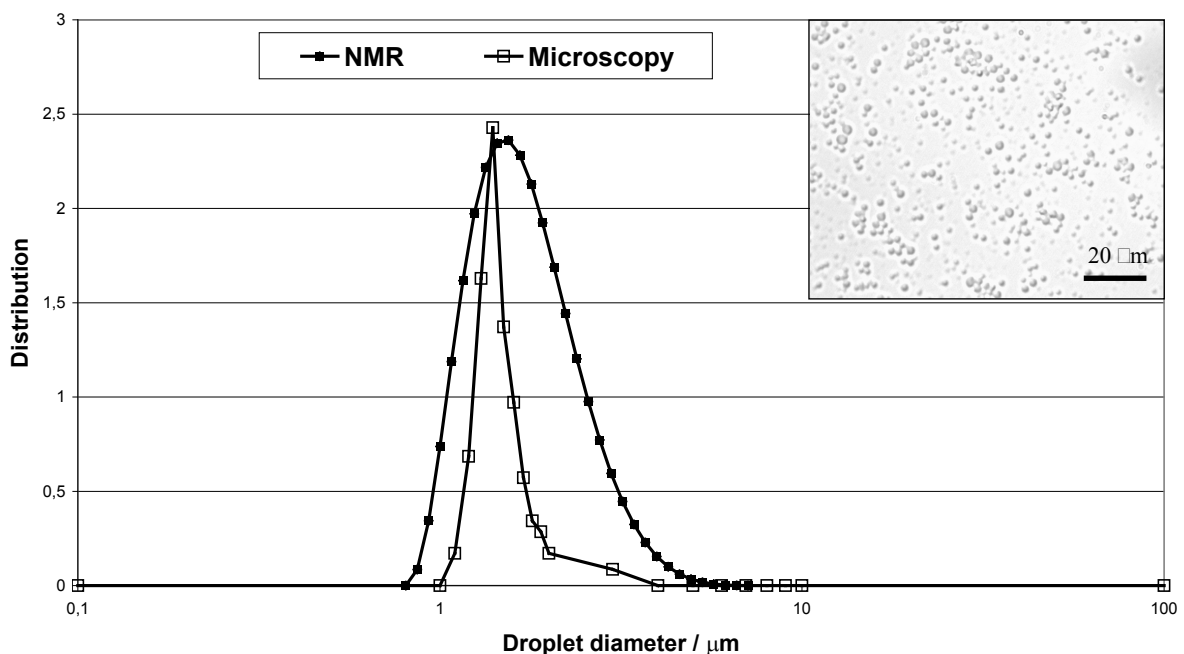


Figure 4.2 Comparison between *DSD*_{asymptotic} ('+') and microscopy ('□')

4.3 On the use of the NMR method for measuring *DSD* in a brine in oil emulsion containing low viscosity oil phase.

When measuring the brine in decane system we realized that there was a strong Δ dependency on the measured *DSD*. As the sequence used was a convection compensated sequence, it was not likely to arise from sedimentation of the droplets, but more a brownian movement of the droplets themselves. As the droplets turned out to be quite small, the thermal movement of the droplets is likely to appear when they are confined in low viscosity oil as decane.

In figure 4.3 we plot the average droplet diameter for the two emulsion systems investigated as a function of the square root of Δ . The emulsion system containing the low viscosity oil exhibit a strong dependency of Δ down to approximately 50 ms, then it levels out. Measurements below 25 ms are not conducted as one then is leaving the regime where the asymptotic approach is valid ($X_{DSD} \ll X_{bulk}$), i.e the apparent measured droplet diameter starts to increase. Therefore care must be taken when choosing Δ for determining the average squared droplet radius, and it is probably wise to check for several Δ -values. Indeed, if brine droplets were allowed to move freely one would expect a linear dependency of measured root of the mean squared displacement, but in figure it reaches a plateau value. This is probably due to the fact that the system measured on had water cut of 60% and it continued to sediment until it had a closed sphere packing of 70% brine droplets. Thus the picture of brownian movement only does not fit to the system. The impact of the packing of the spheres must be taken into account, but is addressed further here.

We also see a small dependency of Δ on the emulsion with high viscosity oil. However this is not due to movement of the droplet, but more likely an effect of a finite width of the relaxation times. The measured droplet diameter is fairly constant up to $\Delta \approx 0.5$ seconds but then starts to increase slightly. As the T_l relaxation times of the brine phase is centred around 1 second, the average droplet diameter will be biased towards the larger droplets with the largest T_l values, and this is exactly what we seen in figure 4.3. As Δ passes 1 second the measured average droplet diameter increases

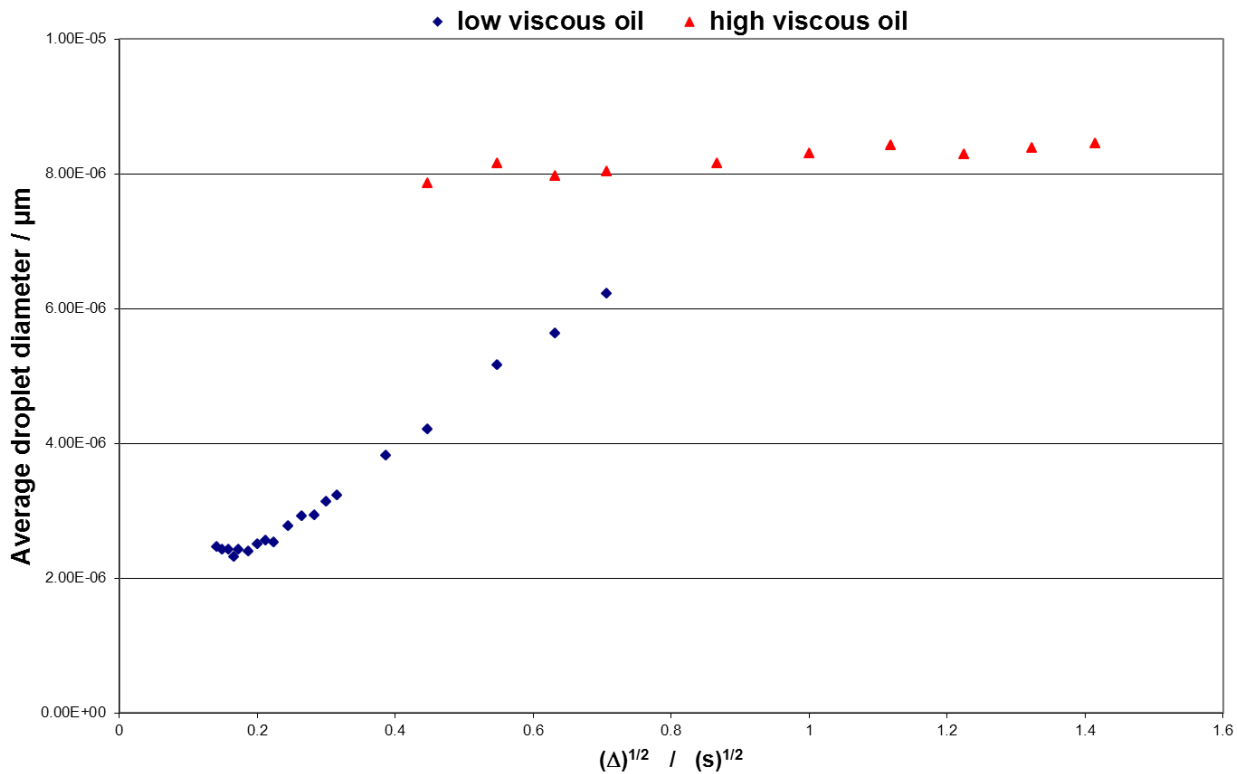


Figure 4.3: Measured volume average droplet radius as a function of observation time Δ

Finally, one should ask what if the droplets were so large that the asymptotic limit (eq. 2.1) was not valid and the movement of the droplets kept us away from reaching the plateau region as shown in figure 4.3? In such a situation it would probably be better to apply the Mitra approach instead [15, 24], but then with a 13 interval PFGSTE sequences in front that is used to suppress low viscosity oil and bulk water. Work is in progress to develop such a method/procedure.

5. Conclusion

A method for fast determination of droplet size distribution of water in oil emulsions is presented, and it returns distributions that are in good agreement with the expected droplet size distribution regardless of the oil viscosity.

References

- [1] Tanner, J.E. and E.O. Stejskal, *The Journal of Chemical Physics*, 1965: p. 288-292.
- [2] Tanner, J.E. and E.O. Stejskal, *The Journal of Chemical Physics*, 1968. 49: p. 1768-1777.
- [3] Goudappel, G.-J.W., J.P.M.v. Duynhoven, and M.M.W. Mooren, *Journal of Colloid and Interface Science*, 2001. 239: p. 535-542.
- [4] Fourel, I., J.P. Guillemin, and D.L. Botlan, *Journal of Colloid and Interface Science*, 1995. 169: p. 119-124.
- [5] Duynhoven, J.P.M.v., et al., *European Journal of Lipid Science and Technology* 2007. 109: p. 1095-1103.
- [6] Kiokias, S., A.A. Reszka, and A. Bot, *International Dairy Journal*, 2004. 14: p. 287-295.
- [7] Aichele, C.P., et al., *Journal of Colloid and Interface Science*, 2007. 315: p. 607-619.
- [8] Packer, K.J. and C. Rees, *Journal of Colloid and Interface Science*, 1972. 40(2): p. 206-218.
- [9] Li, X., J.C. Cox, and R.W. Flumerfelt, *The American Institute of Chemical Engineers Journal*, 1992. 38(10): p. 1671-1674.
- [10] Balinov, B., O. Söderman, and T. Wårnheim, *Journal of the American oil Chemists' Society*, 1994. 71(5): p. 513-518.
- [11] Enden, J.C.v.d., et al., *Journal of Colloid and interface Science*, 1990. 140(1): p. 105-113.
- [12] Callaghan, P.T., K.W. Jolley, and R.S. Humphrey, *Journal of Colloid and Interface Science*, 1983. 93(2): p. 521-529.
- [13] Peña, A.A. and G.J. Hirasaki, *Advances in Colloid and Interface Science*, 2003. 105: p. 103-150.
- [14] R. Bernewitz, G. Guthausen, and H. P. Schuchmann, *Magnetic Resonance in Chemistry*, 2011. 49: p 93-104
- [15] N. van der Tuuk Opedal, G.H.Sørland, and Johan Sjöblom, *Diffusion Fundamentals* 9, 2009, pp 1-29
- [16] G.H. Sørland, *AIP Conference Proceedings Vol. 1330*, 2011, p 27-31
- [17] G. H. Sørland, H. W. Anthonsen, K. Zick, J. Sjöblom, and S. Simon, *Diffusion Fundamentals* 2011, pages 1-9

- [18] H. W. Anthonen, G. H. Sørland, K. Zick, J. Sjöblom, and S. Simon, *Diffusion Fundamentals 2012*, pages: 1-12
- [19] Kärger, J. and D.M. Ruthven, *Diffusion in Zeolites and other Microporous Solids*. 1992, New York: Wiley.
- [20] Balinov, B. and O. Söderman, *Emulsion - the NMR Perspective*. *Encyclopedic Handbook of Emulsion Technology*, ed. J. Sjöblom. 2001, New York: Marcel Dekker.
- [21] Cohen, M.H. and K.S. Mendelson, *Journal of Applied Physics*, 1982. 53: p. 1127
- [22] Uh, J. and A.T. Watson, *Industrial & Engineering chemistry research*, 2004. 43: p. 3026-3032.
- [23] S.W. Provencher *Comput. Phys. Commun.* 27, (1982), 229–242.
- [24] Mitra, P.P., P.N. Sen, and L.M. Schwartz, *Physical Review B*, 1993. 47(14): p. 8565-8574.